Prediction of Fatigue Crack Growth in Railroad Rails

David Broek and Richard C. Rice, Battelle Columbus Laboratories, Columbus, Ohio
Roger K. Steele, Transportation Systems Center, Cambridge, Massachusetts

The objective of this study was the development of a computational model for the prediction of fatigue-crack propagation in rails under train-service loading. Constant-amplitude fatigue-crack-growth properties were determined for 66 rail steels. The effects of mean stress, temperature, and crack orientation were investigated. Variable-amplitude tests showed almost no load-interaction effects in fatigue crack growth in rail steels. Thus a linear integration scheme could be used for crack-growth prediction. Service-simulation tests were performed on the basis of four measured load spectra. The specimens were subjected to random loading, train-by-train loading, loading that used a sequence associated with 170 trains of six different types, and unit-train loading. The load sequence represented 0.9 million gross metric tons (1 million gross tons) of traffic and was repeated until failure of the specimens. Crack growth in the service-simulation tests could be reproduced by using the computational prediction model within a factor of 2 and within a factor of 1.5 in most cases. Discrepancies between predictions and tests results are partially due to the variability of crack-growth properties of rail steels. The way in which the prediction model can be used in a reliability analysis for failure-rate prediction is discussed. Such an analysis would allow management decisions with regard to the most cost-effective means to reduce failure rates of a given track. This is possible because the relative accuracy of the crack-growth prediction is expected to be better than its absolute accuracy.

Fatigue failure of railroad rails is a common cause of derailment accidents. The reduction of fatigue failures can be achieved by more intensive track maintenance, reduction of traffic (loads), or replacement of rails. In addition, timely detection of fatigue cracks through periodic inspection might prevent most cracks from causing failures.

However, measures to reduce fatigue failures will be effective only if there are adequate methods for the prediction of the time to crack initiation and the subsequent rate of crack growth. Such prediction methods require rather accurate information about service loads, rail stresses, and fatigue and crack-growth properties of rail material. Moreover, a computational scheme is required that can use this information to predict behavior under service circumstances.

One portion of the track performance improvement program sponsored by the Federal Railroad Administration is the development of a predictive rail-failure model that can be used for the determination of optimal inspection periods through a calculation of fatigue-crack-propagation behavior. The research reported here concerns a program to develop a computational rail-failure model.

The laboratory fatigue-crack-growth data used as input to the predictive model should be obtained from a sufficiently large sample of rails to manifest the statistical variability. Such data did not exist in the first phase of the program. Data were generated for 66 rail samples of various ages and masses and from various suppliers (1, 2). The samples were taken from existing track in all sections of the United States. Fatigue-crack-growth tests were performed under constant-amplitude loading and zero minimum load.

Actual cracks in rails develop under more complex conditions than constant-amplitude tension loading and zero minimum load. They are subjected to stress histories in which there are varying amplitudes of combined tension and shear that cover a wide range of mean stresses. Cracks can initiate in different sections of the rail and have different orientations; they are internal flaws of predominantly quasi-elliptical shape. Moreover, the rail is subjected to varying temperatures, which may affect the behavior of cracks. A predictive failure model should be cognizant of these complex circumstances. Therefore, data are required on the influences of the various parameters on crack growth. Such data were generated during the second phase of the program.

In the third phase of the program, the predictive failure model was developed. For this purpose, experiments were performed under service-simulation loading. On the basis of these experiments, a crack-growth integration model was established that gives predictions of sufficient accuracy to be within the normal variability of crack growth as observed in the first and second phases of the program.

CRACK-GROWTH PROPERTIES OF RAIL STEELS (PHASES 1 AND 2)

Experiments

A total of 66 rail samples were collected from track all over the United States. The samples were characterized with regard to mass, year of production, chemical composition, and mechanical properties. A brief summary of the variability of the data is given below (1 mm = 0.04 in and 1 MPa = 145 lbf/in^2).

Variable	Value			SD	
	Low	High	Mean	Value	Percent of Mean
Carbon, %	0.57	0.85	0.76	0.06	8
Manganese, %	0.61	1.48	0.88	0.17	20
Sulfur, %	0.014	0.052	0.229	0.010	34
Grain diameter, mm	0.066	0.0120	0.087	0.021	25
Pearlite interlamellar spacing	2470	4160	3211	632	20
Tensile ultimate strength, MPa	766	980	918	5.5	4
Tensile yield strength, MPa	414	566	504	5	7
Crack-growth life, log cycles	5.18	6.22	5.68	0.30	5

In phase 1, one crack-propagation specimen was cut from each rail sample. All specimens were subjected to the same cyclic loads at R = 0 where R = ratio between minimum and maximum load in a cycle. This allowed a judgment of the variability of crack-growth properties of the various rail steels.

In phase 2, more detailed tests were performed on a number of rail samples. These experiments included the following:

1. Tests at positive and negative R-ratios;
2. Tests at -40, 21, and 60°C (-40, 70, and 140°F);
3. Tests on cracks of different orientations;
4. Threshold tests (determination of threshold conditions below which fatigue cracks do not propagate);
5. Tests on semielliptical cracks; and

6. Tests under combined tension and shear.

The majority of the specimens were of the compact-tension type. Where such specimens were not suitable (e.g., in the case of negative R-ratio), different types of specimens were used. Figure 1 shows the specimens and the way in which they were taken from the rail. All specimens were machined to 1.25 cm (0.5 in) thick. The planar dimensions of the compact-tension specimens were determined according to ASTM E 399, with W = 7.6 cm (3.0 in). In the following discussion, the coding of specimens as defined in Figure 1 will be used for identification. Rail samples were numbered 001 to 066.

Crack-growth experiments were performed in servo-controlled fatigue machines. Records were made of the crack size (a) as a function of the number of load cycles (N). The rate of crack growth (da/dN) can be calculated easily from these records.

Data Presentation

The crack-growth records of the various types of specimens are not directly comparable, nor are they directly applicable to the case of a crack in a rail. The correlation between cracks of different types can be made only if their crack-growth data can be expressed in a unique way that is independent of the crack size and specimen geometry.

Cracks of different types can be correlated on the basis of the stress-intensity factor (K), which for any crack loaded in tension can be expressed as

$$K = \beta\sigma(\pi a)^{1/2} \quad (1)$$

where σ = remote stress and β = factor that depends on sample geometry (3). If we consider a case for which $\beta = 1$, it follows that two cracks (a_1) and (a_2) that have $a_1 = 4a_2$ will have the same stress intensity if a_2 is subjected to twice as high a stress as a_1. The geometric factors (β) are known for all specimen types used in this program. Geometric factors for actual rail cracks were computed in a parallel program on stress analysis of rails.

The K-value fully describes the entire stress field at the tip of a crack. Thus, if two cracks have the same K-value, they will have equal stress fields at their tips, regardless of σ, β, or a. If two cracks have the same tip stress field, their behavior will be the same. Hence, two cracks that have the same K-value will exhibit equal rates of crack growth:

$$da/dN = f(\Delta K) \quad (2)$$

where ΔK = range of stress intensity during one cycle of loading (minimum load to maximum load).

Equation 2 provides the ability to correlate data about different types of specimens, provided β is known for the rail crack. Therefore, the crack-growth data of the rail steels will be presented in accordance with Equation 2; i.e., the measured crack-growth rates will be presented as a function of ΔK.

Variability of Crack-Growth (Phase 1)

In phase 1 of this program, one constant-amplitude fatigue-crack propagation (FCP) test was completed on each of the 66 samples. Data on some individual samples and the scatter band of all 66 are shown in Figure 2.

The cracking behavior from one specimen to the next was rather variable—the number of cycles required to grow a crack from 25 mm (1.00 in) to failure ranged from 150 000 to more than 2 000 000. These crack-growth lives were statistically analyzed.

The entire collection of data can be described by a single normal distribution. Figure 3 shows the ranking of fatigue lives versus the predicted failure percentages for a log-normal distribution. The ratio of the logarithmic SD of the 66 data points to the logarithmic mean value of the population (commonly called the coefficient of variation) is about 0.053 (5.3 percent).

An attempt to correlate crack-growth behavior with other mechanical properties, chemical composition, and microstructural parameters was made, but no correlations were found, apart from a weak correlation with hardness.

The variability of all parameters for the 66 rail samples is given above. Despite the large variations in chemical composition, the bulk properties (tensile strength and yield stress) do not vary much. The coefficient of variation of the chemical composition is on the order of 10 percent or more. This number is only a few percent for the mechanical properties and, more important, also for the log life. Apparently, the large variations in chemical and structural parameters are not reflected in the variability of the crack-growth life.

Chemical composition and mechanical properties are bulk properties; i.e., they are averages for a large conglomerate of grains, pearlite colonies, and inclusions. Fatigue-crack growth is a very local phenomenon. In each cycle, the crack propagates over a small distance that may vary from 10^{-3} to 10^{-2} mm (10^{-7} to 10^{-4} in), so that only an extremely small amount of material is affected at a given time. Therefore, the variability in crack growth is more a function of local variations in structural and chemical composition. As a consequence, correlations with bulk material properties are not obvious or easily assessable. Another consequence is that the variability of crack-growth properties within a material can be almost as large as the variability among materials of the same type (i.e., variability within one rail as opposed to variability among rails).

Results of Detail Tests (Phase 2)

The overall data trends for the room-temperature crack-growth experiments on LT orientation specimens are shown in Figure 4. Three distinct bands are formed for each stress ratio when the data are plotted against ΔK. Trend lines for the effects of orientation and temperature are shown in Figures 5 and 6. There appeared to be no discernable effect of cycling frequency on crack growth.

Threshold experiments were done at three stress ratios (R = -1.0, 0.0, and 0.50) to develop estimates of threshold stress-intensity levels below which crack-growth rates would asymptotically approach zero. The results of these tests are reflected in the trend lines in Figures 4, 5, and 6, which show that the crack-growth rates become extremely low at a given ΔK level. If the crack becomes long, the conditions for final failure are approached. Therefore, the crack-growth rate tends to infinity at high ΔK levels. This results in the typical sigmoidal shape of the rate curves shown in Figures 4, 5, and 6.

If the data are to be used for predictive purposes, it is beneficial to use an equation that fits the data. Data sets for a limited range of ΔK values (such as those in Figure 2) often can be described by a straight line on a double-log plot. This leads to the simple relationship

$$da/dN = C\Delta K^m \quad (3)$$

Obviously, this equation is inadequate if the complete sigmoidal curve must be represented.

Many theoretical and empirical relationships have been proposed for the rate curve. Because none of these equations has a sound physical basis, it is often more useful to determine an empirical equation that fits the data for a particular application. This provides the best guarantee of technically adequate predictions.

It was found that a further development of some existing equations was the best suited to the rail-steel data generated here. The equation reads

$$da/dN = C(1 - R)^2 (K_{max}^2 - K_{th}^2)[K_{max}^n/(K_c - K_{max})] \quad (4)$$

where

K_{max} = maximum stress intensity in a cycle = $\Delta K/(1-R)$,
K_{th} = threshold stress intensity, and
K_c = critical stress intensity that causes final fracture and, if $R < 0$, its value should be taken as zero.

Note that K_{th} and K_c are the asymptotes of the sigmoidal curve.

To show the adequacy of Equation 4, the trend lines for the LT orientation and room temperature and the points predicted by Equation 4 are replotted in Figure 7. The generality of Equation 4 was shown by the similar plots for different orientations and temperatures. The equation was used as a basis for crack-growth predictions as discussed below.

Figure 1. Orientation of specimens.

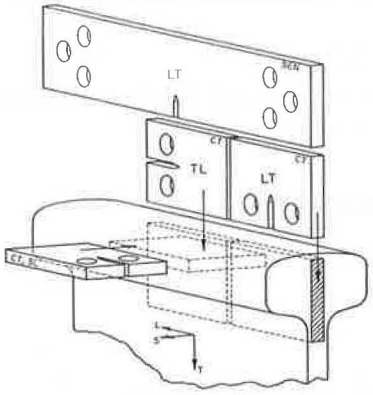

FAILURE MODEL (PHASE 3)

Objective and Scope

The objective of the program was to establish a computational failure model for the prediction of the growth of a flaw in a rail under actual service loading. Flaw growth in a rail is a complex problem; a quasi-elliptical flaw embedded in a nonuniform stress field is growing under a variable-amplitude load history. Probably the most difficult aspect of the problem is the prediction of flaw growth under variable-amplitude loading. This problem was first singled out by the study of a through-the-thickness crack that has a straight front growing under simulated service loading. Once crack growth under these circumstances can be properly predicted, the failure model can be generalized to include the other complexities.

Figure 2. Fatigue-crack-propagation rate behavior: 66 rail samples tested at R = 0.

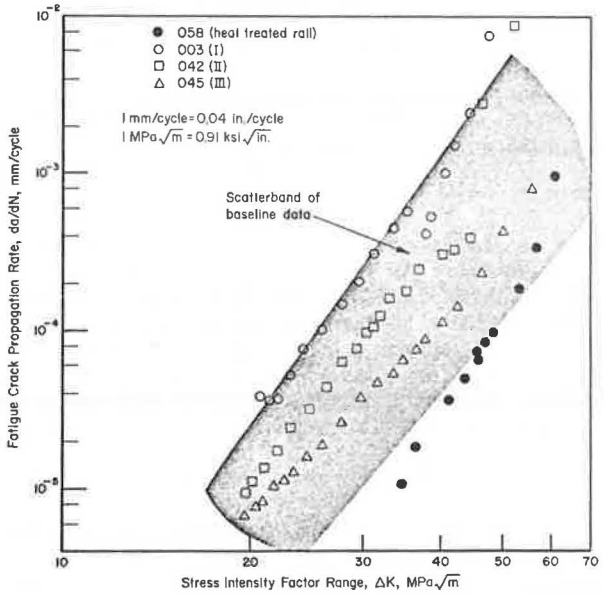

Figure 3. Distribution of baseline FCP lives: 64 rail samples.

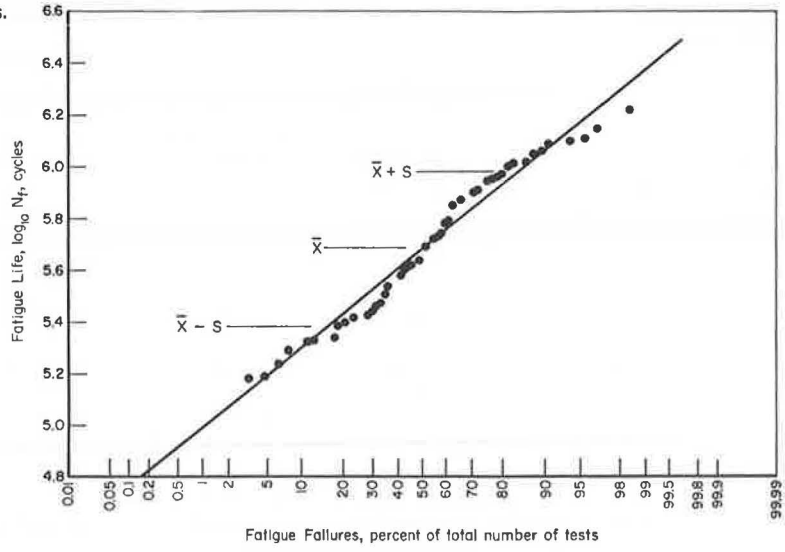

Figure 4. Bands of data variability: LT orientation rail samples at room temperature.

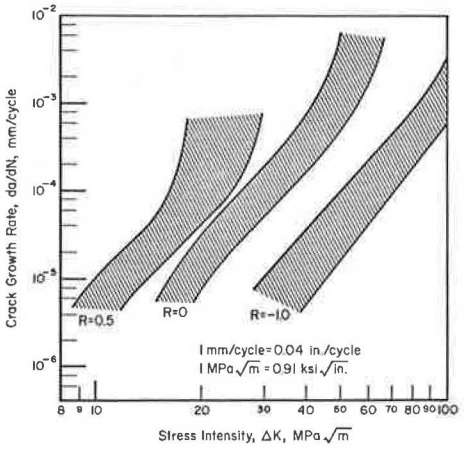

Figure 5. FCP trend lines: rail samples tested at room temperature in three different orientations.

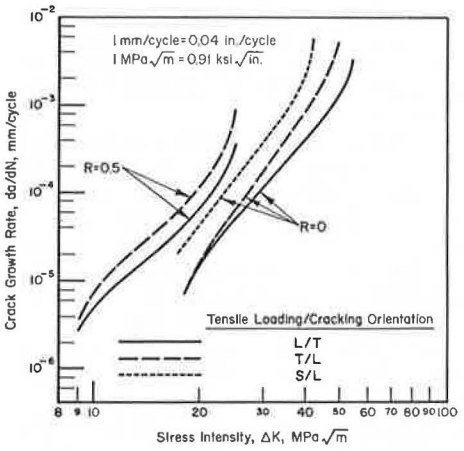

Figure 6. FCP trend lines: LT orientation rail samples at three temperatures and R-ratios.

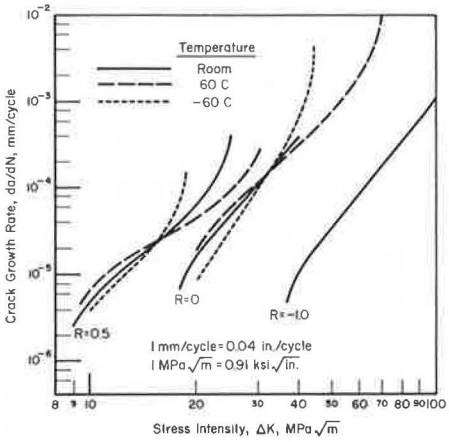

Figure 7. Applicability of crack-growth equations: LT orientation rail samples at room temperature.

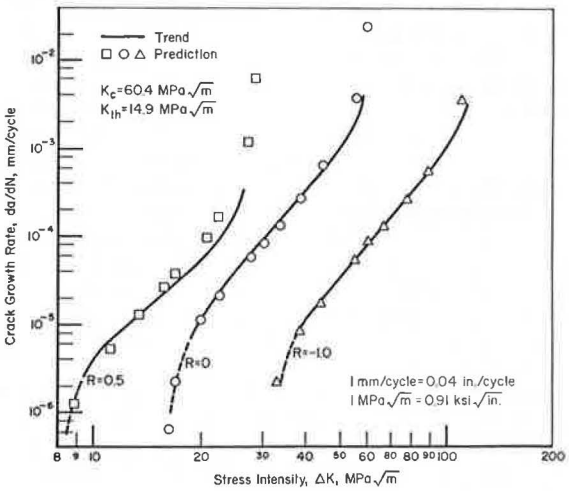

Load Interaction

An important problem in crack-growth prediction is caused by load interaction. In many materials, load interaction will occur if high loads are interspersed among a sequence of low loads. If a high load is followed by a series of loads of lower magnitude, the rate of crack growth can be much lower than if the high load does not occur. This phenomenon is called retardation.

During the application of the high load, a relatively large region of the material around the crack tip is deformed plastically. On unloading, the elastic strains in the surrounding elastic material are reduced to zero. Because the plastic zone at the crack tip is completely contained in elastic material, it has to follow the elastic surroundings during unloading. The plastic strains cannot be (fully) relieved. Thus, a system of residual compressive stresses will develop in the plastic zone at the crack tip when the high load is released and, during subsequent cycling at low loads, the effective stress at the crack tip is reduced because of the presence of the compressive residual stress. As a result, the subsequent loads are less effective in producing crack growth, which means lower crack-growth rates.

Various models have been developed to account for retardation in crack-growth predictions. In the case of random-service loading, crack-growth predictions then have to be based on a cycle-by-cycle integration of growth rates. This is a costly and time-consuming procedure.

A number of rail specimens were subjected to constant-amplitude crack-growth tests in which periodically higher loads of various magnitudes were applied. (The number of high loads was so small that they contributed very little to crack growth.) It was found that rail steels show very little retardation. The crack-growth rates before and after the overloads were virtually the same, and they were no different from the data obtained in experiments that did not have overloads. Therefore, crack-growth prediction in rail steels is not complicated by load interaction effects.

Stresses in the Rail Due to Wheel Passage

In a parallel program, an engineering stress analysis was made of a cracked rail. At the time that the variable-amplitude tests were designed, stress-analysis results were available for an elliptical transverse crack in the rail head. The crack was located approximately in the center of the rail head. The rail was subjected to the passage of a truck that had a wheel load of 84 kN (19 000 lbf). The variation of the mode I stress intensity (K_I) at the lower extremity of the crack is shown in Figure 8.

Initially, when the wheel is still far away, the stress

intensity increases. When the wheel passes over the crack, the rail head is under compressive stress, which causes the stress intensity to decrease. When there is no wheel load on the rail, the only stress in the rail head is the residual stress. It was determined in the rail stress-analysis program that the residual stress at the location of the crack was a tensile stress. Thus, the variation of the stress intensity due to wheel passage is superposed on the positive stress intensity, and the main variation is from the residual stress intensity downward.

A number of load sequences was designed to evaluate the significance of the various small reversals of K_I when a wheel passes. These load sequences are denoted A, B, C, D, E, and F and are shown in Figure 9. The small variations at the top of the cycle have a range that is 15 percent of the total range of the cycle. Because the rate of crack growth is approximately proportional to the fourth power of ΔK, these small variations will contribute 5 percent of the total crack growth. If they are smaller than the threshold, they will not contribute. To evaluate the relative significance of these small load variations, sequences A, B, and C were repeated continuously in a test to simulate the passage of a succession of cars of the same load. Load sequences D, E, and F are self-explanatory.

The most significant results of the sequence tests are shown in Figure 10. Sequences D, E, and F were all run on the same rail sample (025). The results indicate that the small load variations during a wheel pass are insignificant. Therefore, the passage of a truck can be simulated by the two large cycles only (compare sequences D and E). The results for sequence A on rail sample 065 again show the considerable variability of crack growth within one rail sample, even under variable-amplitude loading. This indicates that the results of sequences D, E, and F are equivalent for all practical purposes.

The absence of retardation indicates that a linear integration of crack growth can be sufficient for crack-growth predictions. The results for sequences E and F indicate that it is permissible to combine considerable size blocks of equal cycles, which facilitates the integration procedure.

Rail Service Loading

Actual service-load spectra were obtained from a parallel program on wheel-rail load measurements. Cumulative probability curves are given in Figure 11 for four different railroads (I, II, III, and IV). The spectra are peak counts of measured load histories and show the probability that a certain wheel load is exceeded.

A combination of the I and II spectra was used as the basic spectrum for the service-simulation tests. For this purpose, a load exceedance diagram for 0.9 million gross metric tons (MGMT) (1 million gross tons) of traffic was generated in the following way:

For estimating purposes, 3700 axle passes (peak-load occurrences)/d represent an annual traffic of about 18 MGMT (20 million gross tons). This means that $365 \times 3700 \div 20 = 67\,000$ axles represent 0.9 MGMT. It is assumed that half the traffic is based on spectrum I and half is based on spectrum II, which is 33 500 axles each. The load spectrum was converted into a stress spectrum by taking a stress excursion of 1.45 MPa (210 lbf/in^2) per 4.4-kN (1000-lbf) wheel load. This choice was made to obtain reasonable lives of the test specimens. Because of the generality of the concept of the characterization of crack growth on the basis of ΔK, the selection of an arbitrary stress level for the experiments does not affect the generality of the approach.

For the purposes of analysis and tests, it is necessary to approximate the spectrum by a number of discrete levels. It has been shown for aircraft load histories that 8 to 12 discrete levels are generally adequate (4). The 12 levels selected are shown in Figure 12.

Note that the spectrum was clipped at level 1 at approximately 2 occurrences/MGMT. Higher stress levels may occur; however, they will be rare. One cycle of that level will contribute practically no crack growth as compared with the other 67 000 cycles. Thus, it is impractical to include very high stress levels in experiments. (Of course, these high levels cannot be ignored if the probability of fracture is of concern, but they are unimportant for crack growth if there is little retardation.)

Stress Histories for Predictions and Experiments

The stress history of a rail is extremely complex, and it would be impractical if a prediction of crack growth had to be based on the actual history. In the sequence tests discussed above, it was established that the small load variations occurring during the passage of a wheel can be neglected because they do not contribute to crack growth. One objective of the service-simulation tests discussed below was to investigate whether further simplifications are permissible.

On the basis of the discrete load levels of the spectrum approximation, a stress history was developed that consisted of the six different trains shown in Figure 13. The composition of each of the six trains was selected more or less arbitrarily; however, they resemble actual trains in size and load content. A sequence of two A1 trains, six A2 trains, 12 A3 trains, 120 B-trains, 20 C-trains, and 10 D-trains were mixed in such a way that the heavy and light trains were not clogged together. The mixture of 170 trains was repeated during the tests. Similar procedures were followed by using spectra III and IV in Figure 11. An example of a sequence of trains is shown in Figure 14.

To check whether this simple representation is justified, tests also were run in which the loads of the 170 trains were applied in random order, as will occur in actual service. It was also checked whether further simplifications are possible for prediction purposes, because an efficient prediction scheme requires the simplest possible stress history. On the other hand, the stress history should be realistic in the sense that test results and predictions are representative of actual service conditions.

To evaluate possible simplifications, two other stress histories were developed from the spectrum shown in Figure 12. The first one is based on a reduced number (eight) of stress levels in which stress levels 3 to 10 were combined in pairs to give four new levels, 3 to 6.

Because level 8 (level 12 of the original stress history in Figure 12) has a very small stress range, it will contribute little to crack growth. Therefore, one test case was selected in which the cycles of level 12 were omitted. Obviously, this reduces the number of cycles for 0.9 MGMT from 67 000 to 50 000.

Another simplified stress history for the computational scheme would make use of a hypothetical unit train. This means that all 170 trains constituting the 0.9 MGMT are the same: they contain the same load levels and the same number of cycles at each load level. The highest load level that can be applied is the level that is exceeded at least 170 times (because it must occur in every train). The staircase approximation of

Figure 8. K_I history for passage of 84-kN (19 000-lbf) wheel loads on stiff and soft roadbeds for a particular crack geometry and location.

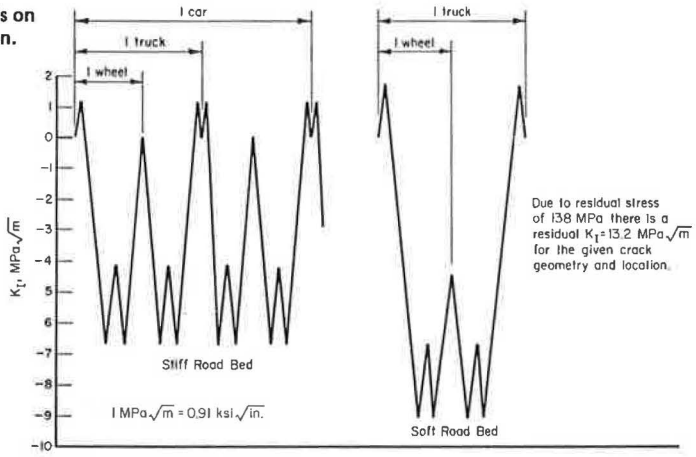

Figure 9. Sequence tests.

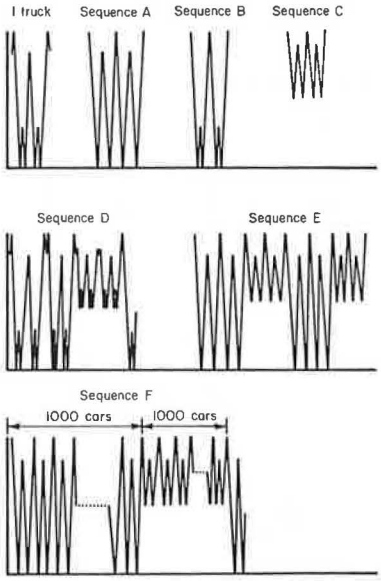

Figure 10. Example of results of sequence tests.

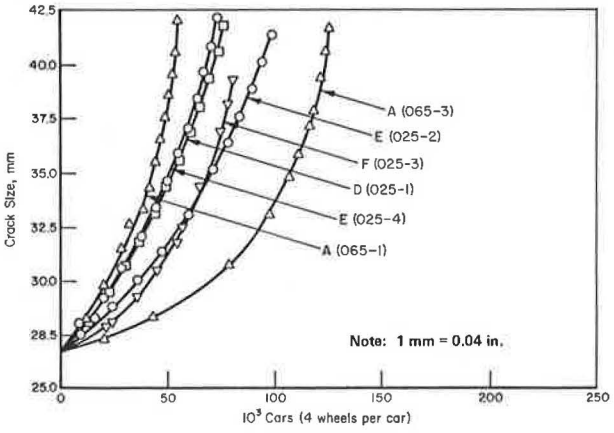

the original spectrum was maintained (Figure 12), but the clipping level was taken at 170 exceedances. The number of cycles at each load level was simply divided by 170 to obtain the number of cycles at each level in the unit train. All loads in the unit train were put in high-low sequence as in Figure 13. Unit trains also were established for spectra III and IV.

Figure 11. Load-probability diagram.

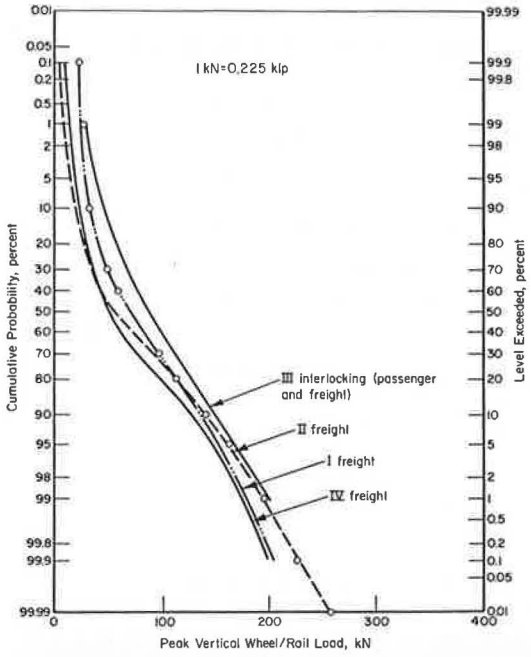

Predictions and Results

Because load interaction did not appear to occur, the service-simulation test data were predicted by integration of the constant-amplitude baseline data without the use of a retardation model. The crack growth (Equation 3) was used as a basis for the integration. Two types of predictions were made. One was based on average crack-growth properties, and the other was based on the constant-amplitude properties of the particular rail sample used for a given service-simulation test.

The integrations were performed numerically. The stress intensity for a certain cycle was calculated, and the crack-growth rate was determined by using Equation 3. If there were k cycles of a given magnitude in a certain train, the total crack growth during those cycles was $\Delta a = \times da/dN$. This crack extension was added to the existing crack. The stress intensity for the next cycle was then calculated, and Δa was determined in the same manner and so on, train after train, until failure.

Predicted curves for the various rail samples and spectra are shown in Figure 15. For a given set of

Figure 12. Stress spectrum for 0.9 MGMT load.

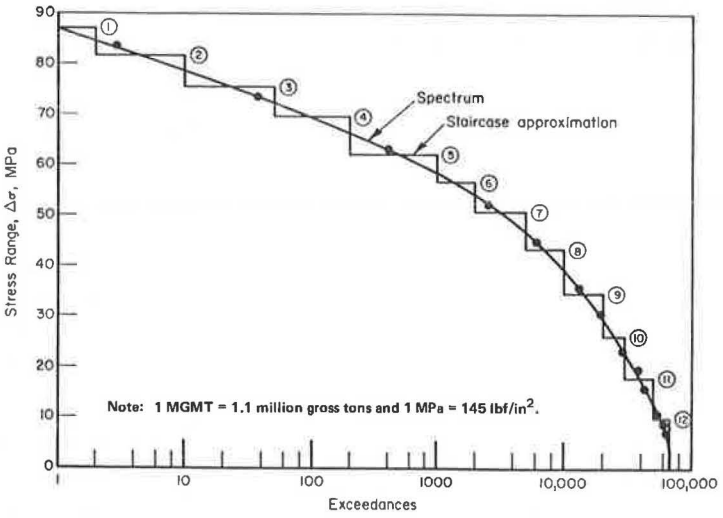

Figure 13. Train compositions for mixed traffic spectrum (all loads included).

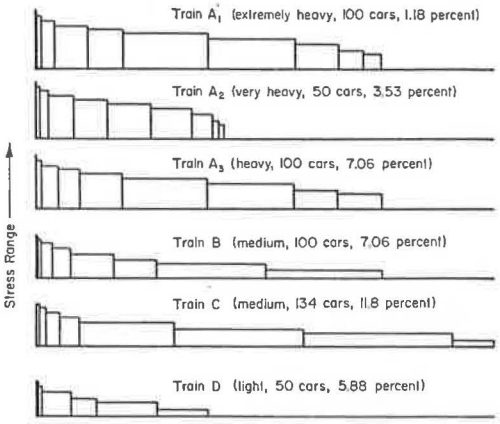

Figure 14. Portion of stress history of 12-level train-by-train service-simulation tests.

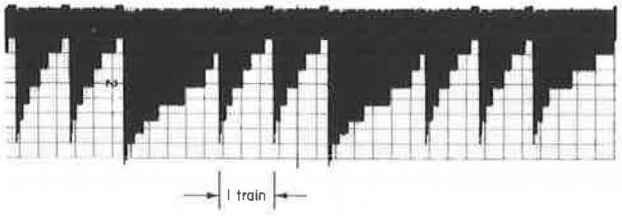

Figure 15. Predicted crack-growth curves.

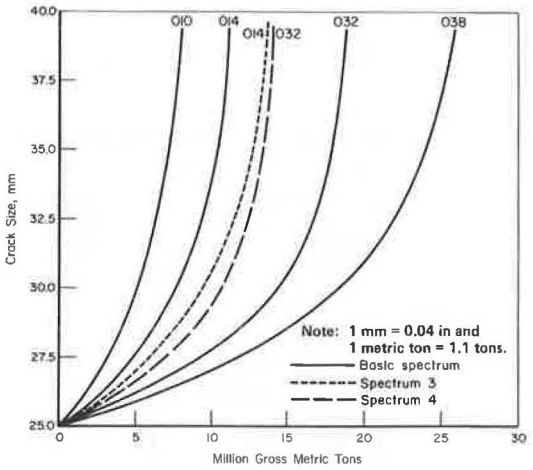

Table 1. Predicted crack-growth life.

Sample No.	Spectrum	Crack-Growth Life (MGMT) 12 Level	8 Level	7 Level	Random	Unit Train
10	Basic	9.1	9.1	9.1	9.1	9.1
14		11.8	10.9	11.8	10.9	11.8
32		19.1	18.2	18.2	18.2	18.2
38		26.4	24.6	25.5	24.6	25.5
14	III	14.6	13.7	13.7	13.7	13.7
18		24.6	22.8	23.7	22.8	23.7
32	IV	14.6	13.7	13.7	13.7	13.7
51		28.2	26.4	27.3	26.4	27.3
20		29.1	27.3	28.2	27.3	28.2
Average data	Basic	11.8	10.9	11.8	11.8	11.8
	III	14.6	13.7	13.7	14.6	13.7
	IV	9.1	9.1	9.1	9.1	9.1

Note: 1 MGMT = 1.1 million gross tons.

data, the computations for 12-level, 8-level, 7-level, and random loading were almost the same, as is shown in Table 1. This indicates that the simplifications are justified for a prediction. Also, the computations for a unit train were almost the same as the others, so that it does not make much difference whether predictions are made by using a random sequence or by using a unit train (which is much simpler).

Of course, it is more important that the predictions agree with the test data. The results of a number of predictions are compared with the actual test data in Figure 16. All predictions and test data are given in Table 2. As can be concluded from these data, the predictions are generally within a multiple of 2, for both the random-loading and the simpler train-by-train simulation tests. This may not be considered very accurate in the light of the more consistent predictions that can be made for aircraft spectra and materials by including the additional complexity of a retardation model (4). However, a look at the actual test data shows that its variability is of the same order of magnitude (compare data that have the same spectrum and the same rail sample), whereas there is no consistent effect of the way the spectrum is approximated. Obviously, if dis-

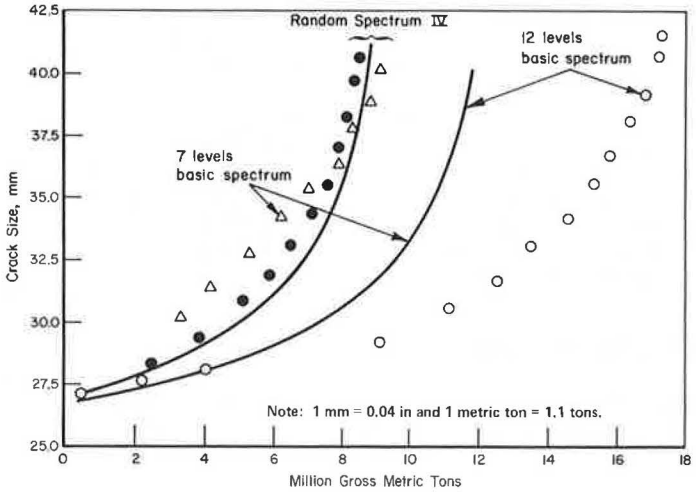

Figure 16. Comparison of predicted and experimental crack-growth curves.

Table 2. Predicted and experimental crack-growth lives.

Sample No.	Spectrum	Type of Loading	Crack-Growth Life[a] (MGMT) Test	Predicted Actual Data	Predicted Avg Data
32	Basic	12 level	18.0	11.8	8.2
	Basic	7 level	10.5	11.8	8.2
38	Basic	8 level	12.0	17.3	8.2
	Basic	Random	12.1	17.3	8.2
14	Basic	8 level	11.7	8.2	8.2
	Basic	Random	17.4	8.2	8.2
14	IV	Random	19.2	9.1	10.9
	IV	Unit train	18.0	9.1	10.0
10	Basic	7 level	12.7	6.4	8.2
32	III	Random	9.2	9.1	7.3
51	III	Random	4.0	15.5	7.3
20	III	Unit train	7.6	15.5	7.3

Note: 1 MGMT = 1.1 million gross tons.
[a] From 27.2 mm (1.07 in) to failure.

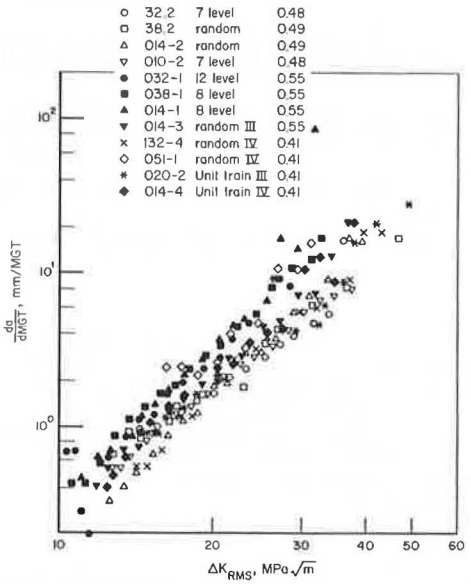

Figure 17. Crack-growth rate per million gross metric tons.

Note: 1 mm/MGT = 0.036 in/million gross tons and 1 MPa$\sqrt{m}$ = 910 (lbf/in^2)$\sqrt{in.}$

crepancies are caused by material variability, they cannot be blamed on the prediction method per se.

As an alternative, it was checked whether the crack-growth rate per 0.9 MGMT of traffic could be expressed uniquely as a function of the root mean square (RMS) value of ΔK. The data for all service-simulation tests are shown in Figure 17. If the data are separated with respect to R-value, a scatter band is found on the order of a factor of 2. This means that predictions within a multiple of 2 also could be obtained by direct integration of data of the type shown in Figure 17.

DISCUSSION AND CONCLUSIONS

These results are a unique and rather complete representation of fatigue-crack-growth properties of rail steels. The effects of R-ratios, orientation, and some other parameters were investigated.

A simple rationale was established to predict behavior under service loading on the basis of constant-amplitude data. This rationale does not give an exact prediction of a particular test result under a particular random sequence of loads, because the variability within a given material cannot be accounted for. However, it does predict the behavior of the family of rail steels to an accuracy within normal material variability. A reliability analysis (or some sort of statistical analysis) then will be required to account for the variability in service.

The combined use of the failure model and a reliability analysis will permit a more rational operation of railroads. For example, consider a railroad in which the number of rail failures is considered unacceptable. The failure model and the reliability analysis are exercised for the particular circumstances of that railroad. The load spectrum is determined for the given traffic and track conditions (a model for spectrum generation is currently being developed). Failure rates are predicted for these circumstances by means of a reliability analysis, which is basically a statistical treatment of the failure model. It is unlikely that the predicted failure rate will be exactly the same as actually experienced.

The question now can be asked: What is the most economical way to reduce this failure rate? To answer this, the reliability analysis is rerun for different conditions [such as (a) reduced speed, (b) reduced traffic, (c) upgraded track, (d) rail replaced, or (e) more frequent inspections]. Each of these measures will reduce the computed failure rate by a certain factor. It then can be decided which measure is the most cost effective.

Because the actual failure rate is known, the reduction factor can be applied to this rate to obtain the actual expected failure rate after one of the measures is carried out.

Thus, the absolute accuracy of the failure model is less important if the trends are predicted properly; i.e., the relative accuracy is more significant. Because all parameters that affect the failure rate (such as material variability and load spectrum) are statistical parameters, a statistical treatment (reliability analysis) is of course necessary.

ACKNOWLEDGMENT

The research described in this paper was performed under contract with the Transportation Systems Center of the Federal Railroad Administration.

REFERENCES

1. C. E. Feddersen, R. D. Buchheit, and D. Broek. Fatigue Crack Propagation in Rail Steels. U.S. Department of Transportation, Rept. DOT-TSC-1076, July 1976.
2. C. E. Feddersen and D. Broek. Fatigue Crack Propagation in Rail Steels. In Standard Testing Procedure 644: Rail Steels—Developments, Processing, and Use (A. H. Stone and G. G. Knupp, eds.), ASTM, May 1978.
3. D. Broek. Elementary Engineering Fracture Mechanics. Nordhoff International Publishing, Leyden, The Netherlands, 1974.
4. D. Broek and S. H. Smith. Spectrum-Loading Fatigue-Crack Growth Predictions and Safety Factors. Naval Air Development Center, Warminster, PA, Rept. No. 76383-30, 1976.

Introduction to Stresses in Rails: Stresses in Midrail Regions

Thomas G. Johns and Kent B. Davies, Battelle Columbus Laboratories, Columbus, Ohio
Donald P. McConnell, Transportation Systems Center, Cambridge, Massachusetts

The results of an extended analysis of the stresses in rails are summarized as an introduction to the mechanisms that drive rail flaws to failure. The mechanics of rail flexural, thermal, contact, and residual stress development are discussed in terms of the distribution of stresses in the rail, the stress cycles that occur with wheel passage, and their relationship to the propagation of typical midrail flaws. These analyses are limited to continuously welded rails and the regions of bolted-joint rails that are outside of the influence of the rail joints.

In recent years, rail failure has ranked as one of the most frequent and costly causes of train derailments (1). Despite substantial programs of inspection and replacement, rail failures remain a significant hazard to the reliability of train operations and a continuing drain on maintenance-of-way budgets. Since the adoption of controlled cooling to prevent hydrogen entrainment by rails and the rail embrittlement that results, a principal concern of railroad engineers has been the stresses induced in the rails by the newest generations of rolling stock. This concern is evident in the writings of Frocht (2) and Code (3) and, most recently, in the report on the problems caused by heavy wheel loads by Way (4) in the Bulletin of the American Railway Engineering Association. This concern is also reflected in the long-standing interest in the analysis of rail stresses that is evident in the literature.

A comprehensive review of approaches to the analysis of the flexural stresses in rails by Kerr (5) has illustrated the historical concern with the complexities of rail behavior under loads. Similarly, the survey by McConnell (6), the recent review of rail stress mechanisms by Johns and Davies (7), and the evaluation of the wheel-rail contact problem by Paul (8) have provided baseline descriptions of the complexities of the stress state in rails that arises from the contact of wheels with the rail and from the residual stresses developed by the yielding of the rail under these severe contact stresses. The interactions between the stresses induced in rails by these mechanisms and the material characteristics of rail steels, which has been discussed by Steele (9), are central to the analysis of the initiation and growth of flaws in rails. Such an analysis is an important part of the evaluation of measures to ensure the reliability of rails in service and to the reduction of the rail failure problem.

In the midrail region (regions between joints), transverse fissures and vertical and horizontal split-head defects (Figure 1) are the principal types of rail fracture. The behavior of these defects when exposed to the railroad load environment is not well understood. However, transverse-fissure defects appear to grow slowly until the defect covers approximately 20 percent of the railhead cross-section area, after which growth becomes rapid and rupture of the entire rail suddenly occurs. A vertical split head may grow to be a meter or so in length before it can be observed on the surface of the rail head. Once an internal crack has reached a free surface, the growth rate normally will increase, but rail fracture will not necessarily immediately occur. A horizontal split-head defect can travel some distance along the rail before turning to run transversely. If both ends of the flaw turn upward, a loss of the running surface results. Alternatively, one end may turn upward and the opposite end turn downward. This results in the type of failure known as a detail fracture. This type of failure is particularly hazardous because it develops rapidly from an embedded horizontal flaw and results in a complete rupture of the rail. As yet, the local stress states that precipitate the branching associated with detail fractures are not well understood.